Liquid Crystals
Publication details, including instructions for authors and subscription information:
http://www.informaworld.com/smpp/title~content=t713926090

Synthesis and characterization of a novel liquid crystal series with tribenzoate cores and monofluoro-substitution on the phenyl ring near the chiral chain

S. Essid[a]; M. Manai[a]; A. Gharbi Corresponding author[a]; J. P. Marcerou[b]; J. C. Rouillon[b]; H. T. Nguyen[b]
[a] Laboratoire de Physique de la Matière Molle, Faculté des Sciences de Tunis, Tunisie [b] Centre de recherche Paul Pascal, Av. Albert-Schweitzer, 33600 Pessac, France

Online publication date: 21 May 2010

To cite this Article Essid, S. , Manai, M. , Gharbi Corresponding author, A. , Marcerou, J. P. , Rouillon, J. C. and Nguyen, H. T.(2004) 'Synthesis and characterization of a novel liquid crystal series with tribenzoate cores and monofluoro-substitution on the phenyl ring near the chiral chain', Liquid Crystals, 31: 9, 1185 — 1193
To link to this Article: DOI: 10.1080/02678290410001648651
URL: http://dx.doi.org/10.1080/02678290410001648651

LIQUID CRYSTALS, VOL. 31, NO. 9, SEPTEMBER 2004, 1185–1193

Synthesis and characterization of a novel liquid crystal series with tribenzoate cores and monofluoro-substitution on the phenyl ring near the chiral chain

S. ESSID, M. MANAI, A. GHARBI*
Laboratoire de Physique de la Matière Molle, Faculté des Sciences de Tunis, 1060 Belvédère Tunis, Tunisie

J. P. MARCEROU, J. C. ROUILLON and H. T. NGUYEN
Centre de recherche Paul Pascal, Av. Albert-Schweitzer, 33600 Pessac, France

(*Received 23 May 2003; in final form 29 September 2003; accepted 4 October 2003*)

Two new chiral series, with benzoate cores and monofluoro-substitution in positions 2 and 3 of the first phenyl ring near the chiral chain, have been synthesized and characterized. The mesomorphic properties have been analysed by optical microscopy, differential scanning calorimetry and electro-optical measurements. The first series (I_c) displays a very rich polymorphism including SmA, SmC^*_α, SmC*, SmC^*_{FI}, SmC^*_A phases, whereas the second (I_b) does not exhibit the SmC^*_A phase, and moreover only displays the SmA phase for short alkoxy chains. The effect of the position of the fluoro substituent and the influence of the alkoxy chain length on the mesomorphic behaviour are discussed.

1. Introduction

Since the discovery of 'antiferroelectricity' in liquid crystals by Chandani *et al.* [1], the SmC^*_A phase has been the focus of much attention, especially for display applications [1–4]. This discovery has also stimulated the search for new materials. A large number of compounds exhibiting these phases have been synthesized and characterized. Several fluoro-substituted benzoate derivatives have been reported by different groups [5–9]. In this study, we explore the influence of fluorine substitution near the chiral chain on the stabilization of tilted mesophases in the series of compounds $\mathbf{I_b}$ and $\mathbf{I_c}$ (the series $\mathbf{I_a}$ without fluorine substitution was reported by Faye *et al.* [6]); these are referred to as C*n*-F3 ($\mathbf{I_b}$) and C*n*-F2 ($\mathbf{I_c}$), where $n = 7$–12. We also discuss the influence of the alkoxy chain length and of the fluorine position on mesophasic behaviour.

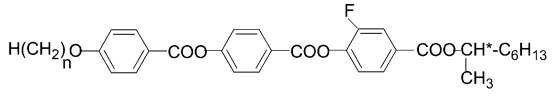

$\mathbf{I_b}$

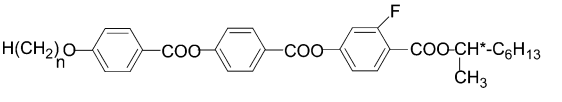

$\mathbf{I_c}$

*Author for correspondence; e-mail: adelhaf.gharbi@fst.rnu.tn

2. Synthesis

The series were prepared following the synthetic pathway shown in the scheme. NMR spectra were recorded on a Bruker HW 200 MHz spectrometer, infrared spectra on a Perkin-Elmer 783 spectrophotometer. The following examples are typical of the synthetic methods used to obtain the compounds given in tables 1 and 2.

2.1. *4-Benzyloxy-3-fluorobenzoic acid (**1b**)*

To a solution of KOH (4.2 g, 0.0075 mol), water (10 ml), ethanol (50 ml) and ethyl 4-hydroxy-3-fluorobenzoate (9.2 g, 0.05 mol) was added dropwise benzyl bromide (6.5 ml, 0.055 mol). The mixture was stirred under reflux for 3 h. After cooling to room temperature, KOH (3.5 g, 0.0625 mol) in water (10 ml) was added and the mixture again stirred under reflux for 2 h. The solvent was evaporated and the residue was hydrolysed with concentrated HCl (12 ml) and water (100 ml). The mixture was stirred for 30 min and the solid filtered, washed with water and crystallized in 95% ethanol. Yield: 9.2 g (74.4%). ^{1}H NMR ($CDCl_3$, ppm): 5.2 (s, 2H,–CH_2–O–), 7.1 (t, 1H arom. *meta* to F), 7.4 (m, 5H arom.), 7.8 (m, 2H, *ortho* and *para* to F). IR (KBr) (cm^{-1}): large signal 2950 (O–H), 1680 (C=O), 1617, 1518, 1450 (C=C phenyl rings).

Liquid Crystals ISSN 0267-8292 print/ISSN 1366-5855 online © 2004 Taylor & Francis Ltd
http://www.tandf.co.uk/journals
DOI: 10.1080/02678290410001648651

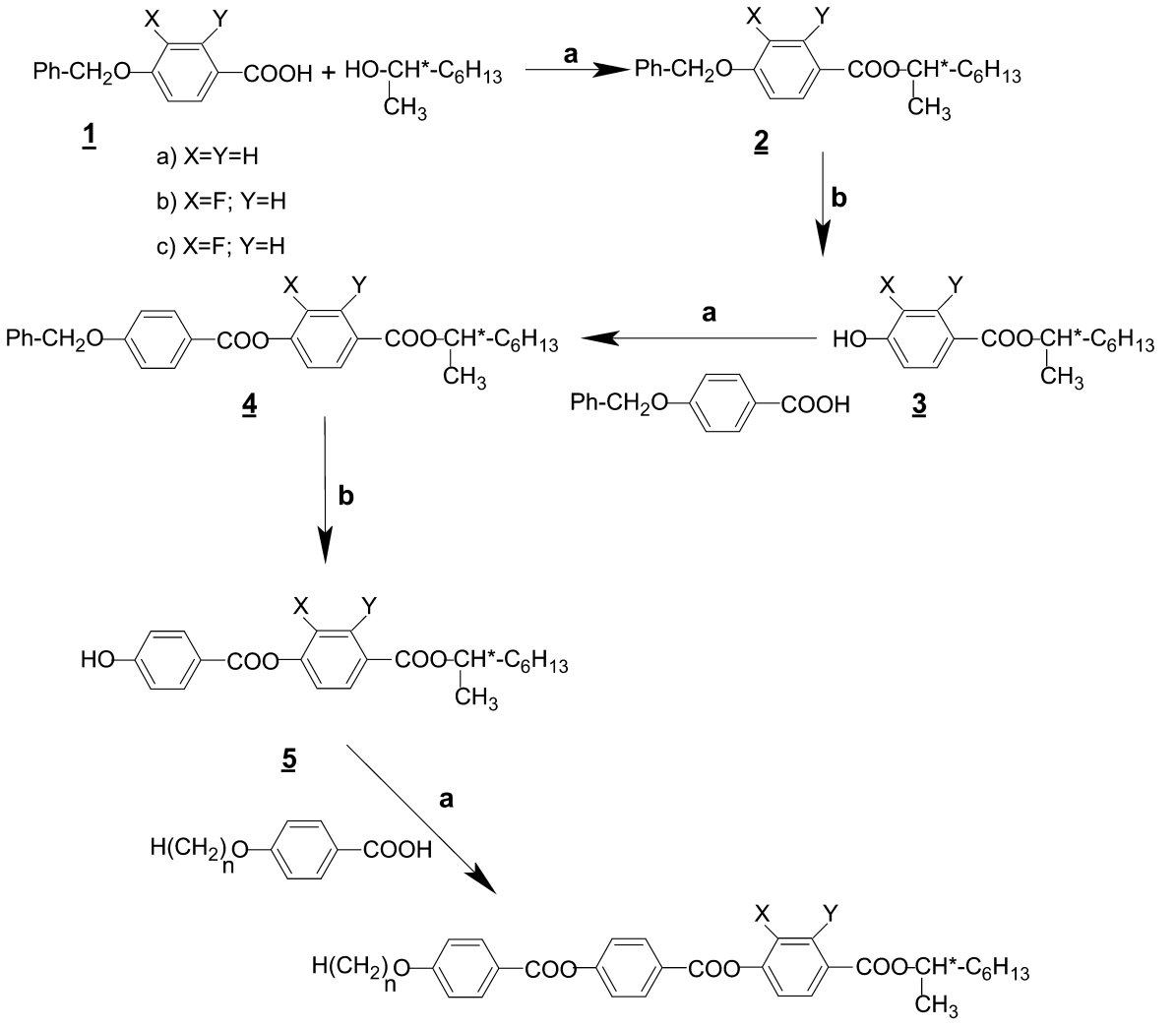

Scheme. Synthetic route to $\mathbf{I_b}$ and $\mathbf{I_c}$ series.

2.2. *4-Benzyloxy-2-fluorobenzoic acid (**1c**)*

This was prepared following the method described elsewhere [7].

2.3. *(R)-1-Methylheptyl 4-benzyloxy-3-fluorobenzoate (**2b**)*

This was prepared following the method described elsewhere [10]. ^{1}H NMR ($CDCl_3$): δ (ppm) = 0.88 (t, 3H, CH_3 of C_6H_{13}), 1.3 (t, 6H, $3CH_2$), 1.36 (d, 3H, CH_3–CH*), 1.6–1.8 (m, 2H, CH_2–CH*O), 5 (s, 2H, CH_2O), 5.1 (m, 1H, CH*–CH_3), 7 (t, 1H arom.), 7.4 (m, 5H arom.), 7.8 (2H arom., *ortho* and *para* to F). IR (cm^{-1}): 2930, 2859, 1709, 1606, 1510, 1251, 847, 771, 696.

2.4. *(R)-1-Methylheptyl 4-hydroxy-3-fluorobenzoate (**3b**)*

This was prepared following the method described elsewhere [10]. ^{1}H NMR ($CDCl_3$): δ (ppm) = 0.88 (t, 3H,

Table 1. Transition temperatures (°C) and enthalpies (in italics, kJ mol^{-1}) of the C*n*-F2 series ($n = 7$–12); heating/cooling rate was 3°C min^{-1}. Cr = crystalline phase; I = isotropic phase; (•) = monotropic transition.

n	Cr		SmC^*_A		SmC^*_{FI}		SmC*		SmC^*_α		SmA		I
7	•	59.4	•	104.5 *0.04*[a]	—		—		•	107.3 *0.03*	•	144.5 *8.45*	•
8	•	62.5 *36.44*	•	111 *0.23*[a]	•	111.2	•	112 *1.4*[b]	•	114.3	•	141.7 *8.3*	•
9	•	79.4 *45.38*	•	115.5 *0.1*[a]	•	117	•	120.4 *0.2*[b]	•	121.8	•	138.6 *7.85*	•
10	•	78.3 *43.84*	•	117 *0.11*[a]	•	119	•	123.3 *0.41*[b]	•	124.4	•	136.8 *7.77*	•
11	•	73.8 *45.42*	•	110.8 *0.08*[a]	•	113.3	•	123.3 *0.61*[b]	•	123.8	•	133.7 *7.51*	•
12	•	63.8 *41.81*	•	109.5 *0.08*[a]	•	112	•	124 *0.81*[b]	•	124.2	•	132.1 *7.4*	•

[a]Combined enthalpies for the transitions SmC^*_A–SmC^*_{FI} and SmC^*_{FI}–SmC*.
[b]Combined enthalpies for the transitions SmC*–SmC^*_α and SmC^*_α–SmA.

CH_3 of C_6H_{13}), 1.3 (t, 6H, $3CH_2$), 1.36 (d, 3H, CH_3–CH*), 1.6–1.8 (m, 2H, CH_2–CH*O), 5.1 (m, 1H, CH*–CH_3), 7 (t, 1H arom.), 7.8 (2H arom., *ortho* and *para* to F). IR (cm^{-1}):3346, 2930, 2859, 1710, 1606, 1510, 1251, 847, 771, 696.

2.5. *(R) 1-Methylheptyl 4-(4-benzyloxybenzoyloxy)-3-fluorobenzoate (**4b**)*

To a solution of (*R*)-1-methylheptyl 4-hydroxy-3-fluorobenzoate (5.36 g, 0.02 mol) in CH_2Cl_2 (100 ml) was added DCC (4.46 g, 0.022 mol), DMAP (0.26 g, 0.026 mol) and compound **1a** (5.0 g, 0.022 mol). The mixture was stirred at room temperature overnight, filtered, the solvent evaporated and the residue purified by chromatography on silica gel using CH_2Cl_2 as eluent. Yield: 6.7 g (66%). ^{1}H NMR ($CDCl_3$): δ (ppm): 0.9 (t, 3H, CH_3 of C_6H_{13}), 1.2–1.5 (m, 11H, $4CH_2$ and CH_3–CHO), 1.6–1.8 (m, 2H, $\underline{CH_2}$–CHO), 5.15 (m, 1H, O–$\underline{CH}$–CH_2–) 5.2 (s, 2H, –CH_2–O–), 7.1 (t,1H arom. *meta* to F), 7.3 (d, 2H, arom.), 7.4 (m, 5H arom.), 7.9 (m, 2H, *ortho* and *para* to F), 8.1 (d, 2H, arom.). IR (KBr) (cm^{-1}): 2958, 2927, 2858 (C–H aliphatic), 1716 (C=O), 1618, 1526, 1440 (C=C phenyl rings), 936 (*para*).

2.6. *(R) 1-Methylheptyl 4-(4-hydroxybenzoyloxy)-3-fluorobenzoate (**5b**)*

To a solution of compound **4b** (8 g, 0,017 mol) dissolved in 200 ml of ethyl acetate was added 1 g of Pd/C. Hydrogen was added under a slight pressure. When the reaction was finished the catalyst was filtered off and the solvent evaporated. As the reaction is quantitative, the liquid phenol was used without further purification.

Table 2. Transition temperatures (°C) and enthalpies (given in italics in kJ mol^{-1}) of the C*n*-F3 series ($n = 7$–12); heating/cooling rate was 3°C min^{-1}. Cr = crystalline phase; I = isotropic phase; (•) = monotropic transition.

n	Cr		SmC^*_{FI}		SmC^*_{FI2}		SmC*		SmC^*_α		SmA		I
7	•	73.8 *34*	—		—		—		—		•	112.8 *4.4*	•
8	•	67.7 *42*	—		—		—		—		•	113 *4.8*	•
9	•	72.7 *46*	—		—		—		(•	63)	•	110 *4.6*	•
10	•	68 *45.4*	—		(•	61)	•	64	•	70 *0.06*	•	108 *4.5*	•
11	•	66 *48.6*	—		•	72	•	81	•	81.7 *0.13*	•	103.8 *4.5*	•
12	•	64 *43.5*	(•	56)	•	71	•	88.5	•	89 *0.19*	•	106 *4.5*	•

Yield: 6 g (91%). ^{1}H NMR ($CDCl_3$): δ (ppm): 0.9 (t, 3H, CH_3 of C_6H_{13}), 1.2–1.5 (m, 11H, $4CH_2$ and CH_3–CHO), 1.6–1.8 (m, 2H, CH_2–CHO), 4.15 (m, 1H, OH), 5.15 (m, 1H, O–CH–CH_2–), 7.1 (t, 1H arom. *meta* to F), 7.3 (d, 2H, arom.), 7.9 (m, 2H, *ortho* and *para* to F), 8.1 (d, 2H, arom.). IR (NaCl) (cm^{-1}): 3346 (O–H), 2956, 2932, 2859 (C–H aliphatic), 1740, 1716 (C=O), 1617, 1604, 1520, 1505, 1440, 1413 (C=C of the two phenyl rings), 931 (*para*).

2.7. *(R)-1-Methylheptyl 4[4-(4-decyloxybenzoyloxy)benzoyloxy]-3-fluorobenzoate (**Ib**)*

To a solution of phenol **5b** (0.194 g, 0.5 mmol) in CH_2Cl_2 (5 ml) was added DCC (0.11 g, 0.55 mmol), DMAP (0.005 g, 0.5 mmol) and 4-decyloxybenzoic acid (0.14 g, 0.5 mmol). The resulting mixture was stirred at room temperature overnight. The solution was filtered, the solvent evaporated. The residue was purified by chromatography on silica gel using CH_2Cl_2 as eluent. The product (white powder) was crystallized from absolute ethanol.Yield: 0.2 g (60%). ^{1}H NMR ($CDCl_3$): δ (ppm): 0.9 (t, 6H, CH_3 of C_6H_{13}, CH_3 of $C_{10}H_{21}$), 1.2–1.5 (m, 25H, $7CH_2$ of $C_{10}H_{21}$, $4CH_2$ and CH_3–CHO), 1.6–1.8 (m, 4H, $2CH_2\beta$), 5.15 (m, 1H, O–CH–CH_2–), 7.1 (t, 1H arom. *meta* to F first ring), 7.25 (t, 1H arom. *meta* to F), 7.3 (d, 2H, arom.), 7.9 (m, 2H, *ortho* and *para* to F first ring), 8 (m, 2H, *ortho* and *para* to F), 8.1 (d, 2H, arom.). IR (KBr) (cm^{-1}): 2953, 2925, 2853 (C–H aliphatic), 1740, 1712 (C=O), 1615, 1513, 1439 (C=C phenyl rings).

3. Mesomorphic properties

The phase behaviour and transition temperatures of the two series were determined using polarizing optical microscopy (POM) (Mettler FP5) and differential scanning calorimetry (Perkin-Elmer DSC 7). Slight differences between these two methods of measurement are, in part, due to instrumental factors and difficulties in distinguishing some transitions. The liquid crystal transition temperatures and enthalpies for these new materials are summarized in tables 1 and 2 and figures 1 and 2. Heating and cooling rates were $3^\circ C\,min^{-1}$. When transition enthalpies were too weak to be detected, the temperature given are those observed by POM.

3.1. *The Cn-F2 series*

3.1.1. *Microscopy observations*

From table 1, it can be seen that the C*n*-F2 series displays the well known sequence SmA, SmC^*_α, SmC*, SmC^*_{FI}, SmC^*_A. On cooling from the isotropic liquid, coloured stripes appear, which grow and curl to form focal-conic fan defects. In addition, the presence of homeotropic domains is characteristic of a SmA phase. The SmC^*_α phase is barely detectable by microscopy because its texture is similar to that of the SmA phase, which may be due to the low tilt angle and helical pitch which increase smoothly with decreasing temperature [11, 12]. The existence of the phase is shown by DSC and with planar aligned samples. The SmC* phase exhibits striated fan-shaped or coloured pseudo-homeotropic domains. Further cooling produces a transition to ferrielectric phases, which show a characteristic texture in the homeotropic part of the cell which moves constantly. We call the phases SmC^*Fi_2 and SmC^*Fi_1. Although they have similar textures and electro-optic behaviour, a transition can be

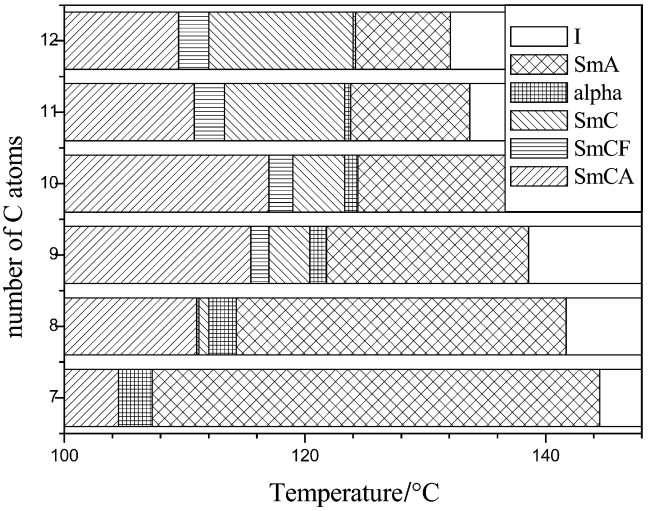

Figure 1. Phase diagrams for the C*n*-F2 series between 100 and 146°C.

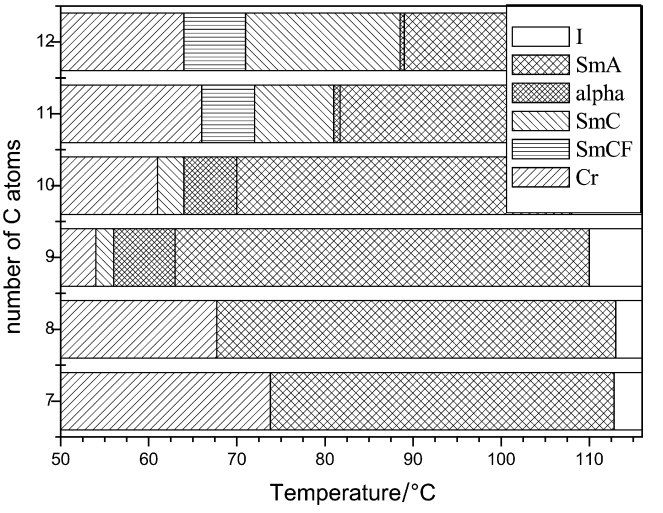

Figure 2. Phase diagrams for the C*n*-F3 series, between 50 and 115°C.

detected between the two phases by DSC (their transition enthalpies are very low, about $0.1\,J\,mol^{-1}$). As the temperature is decreased, the SmC^*_A phase appears, which is similar in appearance to the SmC* phase, showing large stripes growing perpendicular to the rubbing direction. Photomicrographs of these smectic phases are similar to those given in previous articles [13, 14].

3.1.2. *Phase behaviour*

The electro-optical method allows us to complete the characterization and identification of all the transition temperatures. Figure 1 and table 1 show the phase behaviour of the C*n*-F2 series as a function of the alkoxy chain length; we can see that the clearing temperature of the series decreases with increasing chain length. The SmA, SmC^*_α and SmC^*_A phases are present over the whole series from $n=7$ to $n=12$. They follow a similar evolution and their stability decreases on increasing the molecular length. The temperature range of the SmC^*_α phase is very narrow for $n=11$ and 12, about 0.5 and 0.2°C, respectively. Besides the microscopic observations, all the measurements made under a low applied field, show the existence of the SmC* phase. However it disappeared for $n=7$. The ferroelectric phase increases in stability decreasing on the molecular length. The SmC^*_A phase is present over the entire series. A direct SmC^*_A–SmA transition is never observed, and the SmC^*_{FI} phase was usually found above the anticlinic phase, except for $n=7$ for which a direct SmC^*_α–SmC^*_A transition is observed.

3.2. *The Cn-F3 series*

3.2.1. *Microscopy observations*

POM observations of the series are summarized in table 2.

3.2.2. *Phase behaviour*

The phase behaviour of the C*n*-F3 series with different terminal chain lengths is summarized in figure 2. For $n=11$ and 12 on cooling from the isotropic phase, large focal-conic defects develop, characteristic of the SmA phase. This transforms into a broken focal-conic fan-shaped texture. In addition, a colour change of the fans and the appearance of chirality lines were observed, indicating transition to the SmC* phase. The presence of the SmC^*_α phase between the SmA and SmC* phase was expected, but even a study of well planar aligned samples, gave no evidence of this. On further decreasing the temperature, SmC^*_{FI} phases appear which are marked by the typical whitish fluctuating texture in regions of homeotropic alignment. Conoscopic observations under an applied field confirm the existence of this phase.

4. Electro-optic studies

4.1. *Experimental procedure*

All measurements were performed using a classical electro-optical set-up for the measurement of switching current, response time and apparent tilt angle [15]. Electric field-dependent properties of these series have been investigated using commercial cells (EHC, Japan) coated with indium tin oxide. The thickness of the cells was 15 μm, the active area was $25\,mm^2$. Uncertainties in cells spacing are ± 1 μm. The cells were filled with the liquid crystal by capillary action from the isotropic phase, placed in a temperature-controlled oven, and slowly cooled into the SmA phase to avoid the appearance of focal-conic texture [16]. We note that the differences in temperature between the electro-optical and DSC measurements, for all the transition temperatures, were due to the higher rate of heating in the DSC experiments. For the electro-optical study, we used a temperature regulator, consisting of a programmable direct current supply (HP E3632A), a programmable Keithley multimeter (model 2000) and an oven made in our laboratory. The temperature was controlled within 0.01°C accuracy.

4.2. *SmC^*_α response*

On cooling from the isotropic liquid of C10-F3, both SmA and SmC^*_α phases are found. For the electro-optic study we used a triangular wave form, see figure 3. This allows the SmC^*_α phase to be distinguished from the SmC* phase. Thus in the SmC* phase the polarization switches from $-\mathbf{P}$ to $+\mathbf{P}$ leading to a single peak per half–period see figure 3 (*e*, *f*). At the SmC*–SmC^*_α phase transition a second peak appears, its evolution is given by figures 3 (*a–d*). The SmC^*_α phase occurs over 5°C (from 65 to 70°C) for C10-F3 and over 7°C for C9-F3. A comparison between these ranges and those for C10-F2 (1.1°C) and C9-F2 (1.4°C) clearly shows the influence of the position of the fluoro substituent on the existence of the SmC^*_α phase.

4.3. *Temperature dependence of electro-optic parameters*

4.3.1. *Saturated polarization*

These measurements were performed under a rectangular a.c. field ($\nu=41$Hz) at saturation. This polarization was calculated by the integration of the switching current induced in the cell, under the reversal of the applied field. In all the phases, the applied field was strong enough to induce the saturated ferroelectric

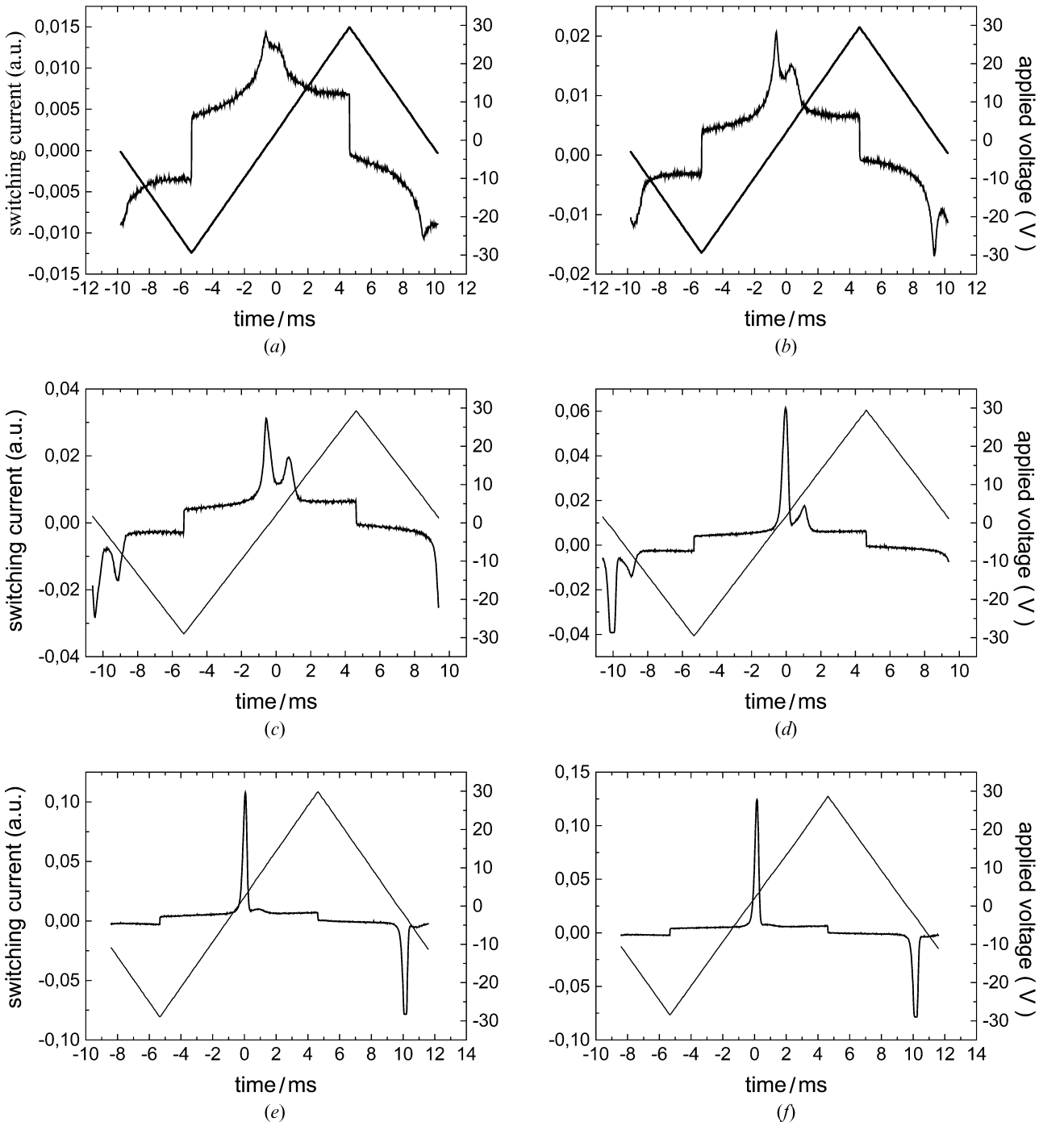

Figure 3. Switching current for the SmC^*_α (*a–d*) and the SmC* (*e*, *f*) phases at $\mathbf{E} = 5.2\,\mathrm{V\,\mu m^{-1}}$, $v = 50\,\mathrm{Hz}$, under a triangular electric field, for C10-F3: (*a*) SmC^*_α at 70°C; (*b*) SmC^*_α at 69°C; (*c*) SmC^*_α at 68°C; (*d*) SmC^*_α phase at 66.5°C; (*e*) SmC^*_α–SmC* transition at 65°C; (*f*) SmC* at 64°C.

state. Under these conditions, we studied the direct FO^+/FO^- switching at various temperatures. Figure 4, shows the behaviour under an a.c. electric field for the compound chosen, $n = 12$. This behaviour is affected by the presence of the fluorine in the first phenyl ring; the curve shows a regular decrease with temperature, with an upper value of $90\,\mathrm{nC\,cm^{-2}}$. As the number of carbons in the alkoxy chain passes from 7 to 12 it raises the polarization value above the SmC^*_A phase (90 instead of $60\,\mathrm{nC\,cm^{-2}}$); these values of saturated polarization are not high and similar to those of many three-ring compounds [5–7].

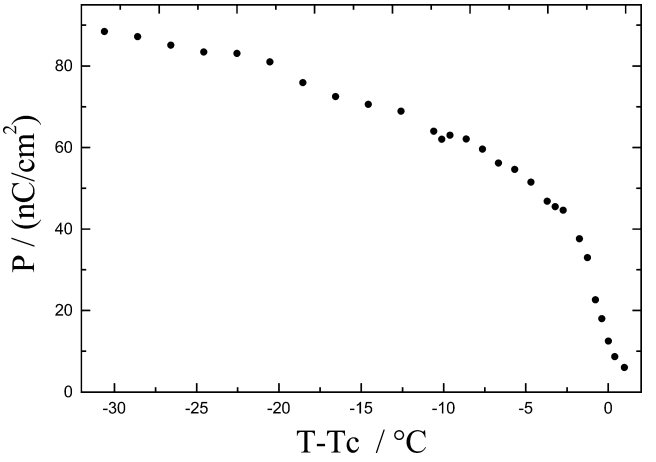

Figure 4. Polarization versus T-T_c at saturation field ($\mathbf{E}=5.3\,\mathrm{V\,\mu m^{-1}}$, $v=41$ Hz) for C12-F2. $T_c=T_{\mathrm{SmA-SmC^*_\alpha}}$ is the $\mathrm{SmA-SmC^*_\alpha}$ transition temperature in the absence of the electric field.

4.3.2. *Response time*

The electric response time is the time required for the majority of the molecules to switch under an a.c. field. It corresponds to the top of the polarization peak. The switching time τ is inversely proportional to the applied electric field $\mathbf{E}$ and the polarisation $\mathbf{P}$:

$$\tau=\frac{\gamma}{\mathbf{PE}}, \text{ where } \gamma \text{ is the rotational viscosity.}$$

The same conditions as for the measurement of the polarization are applied. In figure 5, we show the variation of the response time with temperature at the same saturation field. The decrease of response time with increasing temperature is due to the accompanying decrease of viscosity.

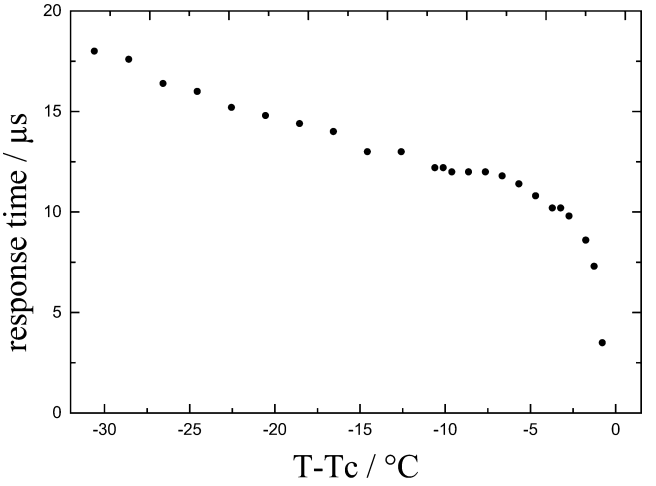

Figure 5. Response time versus T-T_c at saturation field ($\mathbf{E}=5.3\,\mathrm{V\,\mu m^{-1}}$, $v=41$ Hz) for C12-F2.

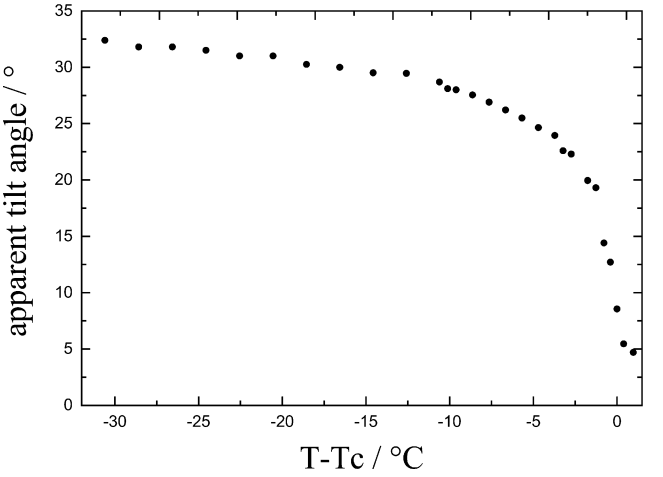

Figure 6. Apparent tilt angle versus T-T_c at saturation field ($\mathbf{E}=5.3\,\mathrm{V\,\mu m^{-1}}$, $v=0.2$ Hz) for C12-F2.

4.3.3. *Apparent tilt angle*

The apparent tilt angle θ was measured with the same field as for the polarization measurements but at very low frequency (0.2 Hz), using the usual 2θ optical method [17]. To determine this parameter we observed the planar-aligned sample through the polarizing microscope. The microscope stage was rotated to obtain extinction of transmitted light in the presence of a large applied electric field ($\mathbf{E}_{\mathrm{sat}}$); measurement accuracy is estimated to be $\pm 0.5^\circ$. The dependence of the tilt angle on temperature for C12-F2 is shown in figure 6; this angle reaches 33° for C12-F2 and 19.5° for C7-F2.

4.4. *Applied a.c. field dependence*

The $\mathrm{SmC^*_A}$ phase requires a relatively high field to accomplish the transition to the ferroelectric phase. This threshold field decreases while the temperature increases (see figure 7). In $\mathrm{SmC^*_{FI}}$ phases, the behaviour is similar, but at low field the polarization reaches a step at approximately $\mathbf{P}/2$. This was previously observed for other types of materials in $\mathrm{SmC^*_{FI}}$ phases [5]. In the SmC* phase, the saturation is easily reached with a field below $1\,\mathrm{V\,\mu m^{-1}}$. This behaviour has been observed previously by many groups [6, 13, 18, 19].

5. Discussion and conclusion

Since the discovery of the anticlinic smectic phase $\mathrm{SmC^*_A}$ [1], several series of compounds have been reported and new examples continue to be synthesized. This work has revealed important parameters that have an influence on the formation and stabilization of this phase, such as the nature and the polarity near the chiral chain. These also have an effect on the electro-optic behaviour.

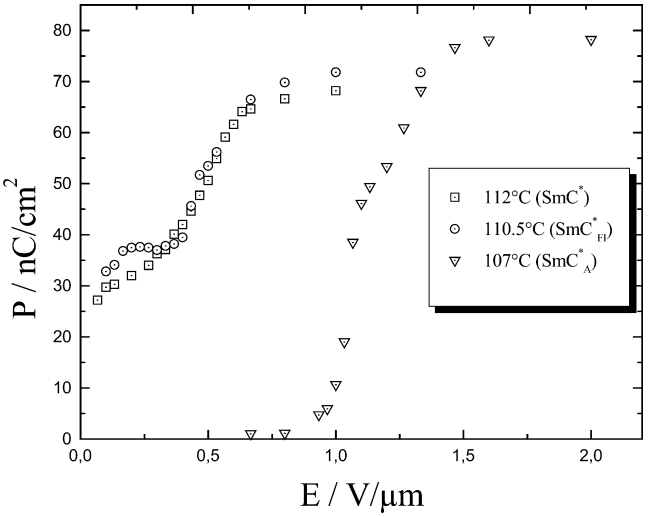

Figure 7. Field dependence of the polarization for C12-F2 at 107, 110.5 and 112°C.

In this paper the synthesis and characterization of two different series, C*n*-F2 and C*n*-F3, have provided several compounds exhibiting a very rich polymorphism, with the formation of SmC^*_A, SmC^*_{FI}, SmC*, SmC^*_α and SmA phases. However moving the fluorine from the 2 to the 3 position causes a marked decrease in the clearing point and transition temperatures of the mesophases. It also affects the mesomorphic behaviour, which indicates clearly the importance of molecular shape. Indeed, we note that the SmC^*_A phase is strongly stabilized in the C*n*-F2 series, while not in the C*n*-F3 series, for which no anticlinic phase was obtained. However the presence of this fluorine is not enough to produce a direct SmC^*_A–SmA transition. Furthermore, the temperature range of the SmC^*_α phase for C9-F3 and C10-F3 (about 6°C) is larger than that of the C*n*-F2 homologues (about 1.3°C).

It is well known that corresponding homologues of the acetylenic series **II** and **III**, have the same total molecular length and the same longitudinal dipole moment, but the local dipole moment is different, giving different mesomorphic sequences. Series **II** does not exhibit anticlinic smectic phases but for long chains exhibits the twist grain boundary smectic A phase (TGB_A) [20, 21].

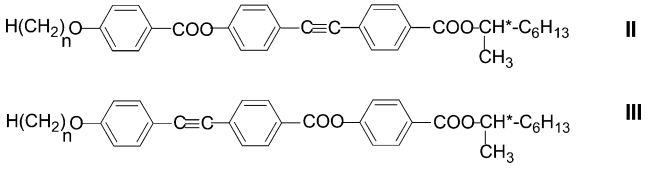

On the other hand, series **III** exhibits different smectic C* subphases [18]. We should note that because

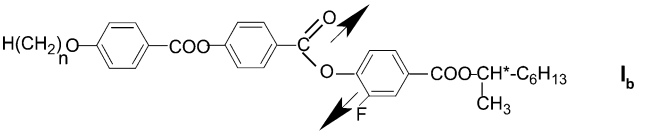

Figure 8. Favourable conformation of $\mathbf{I_b}$ homologues.

of steric hindrance between the fluorine and the COO group, the $\mathbf{I_b}$ series with the fluorine in position 3 has the favourable conformation as shown in figure 8. The local dipole moment between the two phenyl rings nearest to the chiral chain is comparable to that of C≡C of the **II** series. If this analogy is correct, we should obtain the TGB phase for very long chain homologues. Indeed, the octadecyloxy derivative of the $\mathbf{I_b}$ series displays the sequence: Cr 66 SmC* 94 TGB_A 98 I (°C). At a higher temperature than the TGB_A phase, pretransitional effects in the isotropic liquid were seen in the DSC thermogram [22]. By comparison, the $\mathbf{I_c}$ octadecyl homologue only exhibits a SmC* phase: Cr 55 SmC* 115 I (°C).

References

[1] Chandani, A. D. L., Ouchi, Y., Takezoe, H., Fukuda, A., Furukawa, K., and Kichi, A., 1989, *Jpn. J. appl. Phys.*, **28,** 1261.

[2] Yamawaki, M., Yamada, Y., Mori, N., Hayashi, H., Suzuki, Y., Nagi, Y. S., Kawamura, T., and Ishibashi, H., 1989, in Proceedings of the 9 International Displays Research Conference, vol. 3, p. 26.

[3] Yamada, Y., Yamamoto, N., Mori, K., Nakamura, K., Hagiwara, K., Suzuki, Y., Kawamura, I., Orihara, H., and Ishibashi, Y., 1990, *Jpn. J. appl. Phys.*, **29,** 1757.

[4] Johno, M., Chandani, A. D. L., Lee, J., Ouchi, Y., Takezoe, H., Fukuda, A., Itoh, K., and Kitazume, T., 1989, *Proc. Jpn. Display*, 22.

[5] Da Cruz, C., Rouillon, J. C., Marcerou, J. P., Isaert, N., and Nguyen, H. T., 2001, *Liq. Cryst.*, **28,** 125.

[6] Faye, V., Rouillon, J. C., Destrade, C., and Nguyen, H. T., 1995, *Liq. Cryst.*, **19,** 47.

[7] Da Cruz, C., Rouillon, J. C., Marcerou, J. P., Isaert, N., and Nguyen, H. T., 2001, *Liq. Cryst.*, **28,** 1185.

[8] Booth, C. J., Dunmur, D. A., Goodby, J. W., Kang, J. S., and Toyne, K. J., 1994, *J. mater. Chem.*, **4,** 747.

[9] Dong, C. C., Hird, M., and Goodby, J. W., 1996, *Ferroelectrics*, **180,** 245.

[10] Da Cruz, C., Grelet, E., Rouillon, J. C., Marcerou, J. P., Sigaud, G., Pansu, B., and Nguyen, H. T., 2001, *Liq. Cryst.*, **28,** 1415.

[11] Isozaki, T., Hiraoka, K., Takanishi, Y., Takezoe, H., Fukuda, A., Suzuki, Y., and Kawamura, I., 1992, *Liq. Cryst.*, **12,** 59.

[12] Skarabot, M., Cepic, M., Zebs, B., Blinc, R., Heppke, G., Kityk, A. V., and Masevic, I., 1998, *Phys. Rev. E*, **58,** 575.

[13] Nguyen, H. T., Rouillon, J. C., Cluzeau, P.,

SIGAUD, G., DESTRADE, C., and ISAERT, N., 1994, *Liq. Cryst.*, **17,** 571.
[14] GOODBY, J. W., PATEL, J. S., and CHIN, E., 1992, *J. mater. Chem.*, **2,** 197.
[15] DUPONT, L., GLOGAROVA, M., MARCEROU, J. P., NGUYEN, H. T., and DESTADE, C., 1991, *J. Phys. II*, **1,** 831.
[16] ROSENBLATT, C. S., PINDAK, R., CLARK, N. A., and MEYER, R. B., 1977, *J. Phys.*, **38,** 1105.
[17] MARTINOT-LAGARDE, P., DUKE, R., and DURAND, G., 1981, *Mol. Cryst. liq. Cryst.*, **75,** 249.
[18] CLUZEAU, P., NGUYEN, H. T., DESTRADE, C., ISAERT, N., BAROIS, P., and BABEAU, A., 1995, *Mol. Crys. Liq. Cryst.*, **260,** 69.
[19] FAYE, V., ROUILLON, J. C., NGUYEN, H. T., DESTRÉ, L., LAUX, V., and ISAERT, N., 1998, *Liq. Cryst.*, **24,** 747.
[20] NGUYEN, H. T., TWIEG, R. J., NABOR, M. F., ISAERT, N., and DESTRADE, C., 1991, *Ferroelectrics*, **121,** 187.
[21] NGUYEN, H. T., BABEAU, A., ROUILLON, J. C., SIGAUD, G., ISAERT, N., and BOUGRIOUA, F., 1996, *Ferroelectrics*, **177,** 161.
[22] GOODBY, J. W., WAUGH, M. A., STEIN, S. M., CHIN, E., PINDAK, R., and PATEL, J. S., 1989, *Nature*, **337,** 449.